Carbohydrate Research, 232 (1992) 1–15
Elsevier Science Publishers B.V., Amsterdam

Conformational analysis of levanbiose by molecular mechanics *

Jianhua Liu [a] and Andrew L. Waterhouse [b]

[a] *Department of Chemistry, Tulane University, New Orleans, Louisiana 70118 (USA)*
[b] *Department of Viticulture and Enology, University of California, Davis, California 95616 (USA)*

(Received September 3rd, 1991; accepted January 14th, 1992)

ABSTRACT

A relaxed conformational energy map for levanbiose, *O*-β-D-fructofuranosyl-(2 → 6)-β-D-fructofuranoside, was computed with the molecular mechanics program MM2(87). All torsion angles of the three linkage bonds were driven by 30° increments while two primary alcohol groups were held at three staggered forms. The steric energy of all other parameters was optimized. The side groups were retained at the same relative positions on the two rings in this first part of the study so our results are directly applicable to the study of polymeric levan with identical repeating units. The low-energy dimers did not lead to viable polymers. The interresidue linkage torsion angles defined by C-6–O-2′–C-2′–C-1′ (ϕ) and O-5–C-5–C-6–O-2′ (ω) have minima at +60° and −60°, respectively, with accessible minima at other staggered forms. As observed in inulobiose, the preferred torsion angle at central linkage bond defined by C-5–C-6–O-2′–C-2′ (ψ) was antiperiplanar. An analysis of all conformations of staggered side groups showed that the C-1 and C-1′ groups had little effect but the C-6′ group showed a preference for χ-6′(O-5′–C-5′–C-6′–O-6′) = −60°. The fructofuranose rings were started at the low-energy $^{4}_{3}T$ conformation (angle of pseudorotation, $\phi_2 = 265°$) that was retained except when the linkage conformations created severe inter-residue conflict.

INTRODUCTION

Levanbiose (**1**) is the prototype (2 → 6)-β-linked fructofuranose sugar. It can be obtained from controlled acid hydrolysis of the homologous polysaccharide, levan [1], a fructan, and can also be prepared by enzymatic synthesis from fructose [2]. Fructans exist in numerous plants [3] and are a critical carbohydrate source for many plants. The existence of fructans in plants has been correlated with an improved cold-stress response in those plants [4]. Potential industrial, biological, and other uses of levan can be found in a recent review [5].

Correspondence to: Professor A.L. Waterhouse, Department of Viticulture and Enology, University of California, Davis, CA 95616, USA.

* Paper no. 5 of a series: Conformational Analysis of D-fructans.

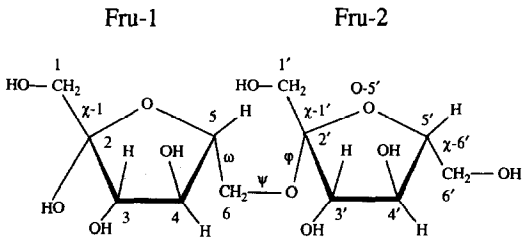

Levanbiose (1)

Fig. 1. Levanbiose (1). ϕ = C-6–O–C-2′–C-1′; ψ = C-5–C-6–O–C-2′; ω = O-5–C-5–C-6–O; χ-1 = O-1–C-1–C-2–O-5; χ-1′ = O-1′–C-1′–C-2′–O-5′; χ-6′ = O-5′–C-5′–C-6′–O-6′.

Fructofuranose rings linked by three bonds are a characteristic of fructans. While most of the attention has been focused on inulin [6–8], the (2 → 1)-β-linked fructan, little is known about the likely conformations of (2 → 6)-β-linked fructan. An X-ray diffraction study of 6-kestose was reported [9]. NMR assignments for grass levan [10] and 6-kestose [11] have been reported. The structure [12] and physicochemical properties [13] of some levans produced by either plant or bacteria have been investigated. The conformational characteristics of levan polymer are largely unknown. While levanbiose can be obtained, experimental conformation of this modeling study may be difficult because experimental solution data is complicated by the presence of multiple forms [14].

In this work, we attempt to determine the steric energy of levanbiose for different values of the torsion angles for the linkage angles ϕ, ψ, and ω, as well as for the three primary alcohol groups. The conformation of the fructofuranose rings also affects the energy values, and while only the low-energy form for the fructofuranose monomer was tested, the ring form was monitored during the analysis.

A study of all three linkage angles and three primary alcohol groups at 30° resolution would require the analysis of 12^6 or 2985984 structures. This is impossible considering computer time alone. To maximize the utility of our results, the number of structures analyzed was reduced by setting χ-1 and χ-1′ to the same angle at the three staggered forms and by keeping χ-6′ the same as ω during Run A (see Fig. 1). These results are thus applicable to levan polymer analysis where the monomer units all adopt the same side-group conformation. We subsequently looked at the side-group positions as a secondary factor.

EXPERIMENTAL

Computational details.—A modified version of MM2(87) was chosen for this study because it has incorporated a new type of dihedral angle driver (option −2)[15], and because it can also drive up to eight angles simultaneously. During the

calculations, the optimization was terminated by the default setting ($\Delta E \leqslant 0.00008N$ kcal/mol, where N is the number of atoms in the molecule). In all tested cases there were no effects found for different dielectric constant settings, so the default (1.5) value was used. The calculated steric energy from MM2(87) was used directly for the comparison of the different conformers and are the energies reported herein. All calculations were carried out on an IBM 3081KX computer. The CPU time for each 12×12 driver calculation was 2–3 h.

The starting structure of **1** was created by using the most-favored monomer conformation ${}^{4}_{3}T$ ($\phi_2 = 265°$) of β-D-fructofuranose [16], and then the geometry was optimized by MM2(87). In the starting structure, ϕ was 52.6°, ψ was 169.6°, ω was 71.6°, χ-1 was 65.7°, χ-1′ was 45.3°, and χ-6′ was −59.2°. The phase angles for the two fructofuranose rings in the starting structure were 266 and 256° for Fru-1 and Fru-2, respectively. No effort was made to search for other possible low-energy ring conformations.

In summary, the conformation analysis was carried out in three steps. Run A: flexible dihedral angle driver analysis of ϕ, ψ, ω, χ-1, χ-1′, and χ-6′. In these computations, only the driven angles were fixed to the desired values. Bond lengths, bond angles, and the non-driven torsion angles were allowed to relax. Run B: using the results from the flexible residue analysis obtained from Run A, fully relaxed structures were generated by reoptimizing the low-energy forms (up to 10 kcal/mol steric energy higher than the minimum found in stage 1) without any restriction. Run C: side-group orientation analysis. Using the lowest energy form found in Run B, χ-1, χ-1′, and χ-6′ were rotated to all combinations of the three staggered positions, and resulting structures were optimized without any restriction.

Run A: taking the starting structure, conformational analysis was carried out by driving ϕ and ψ from −150 to 180° with an increment angle of 30°. In order to accommodate polymer extrapolation, ω and χ-6′ were kept the same and manually set to −150 to 180° at 30° increments using driver specifications. The series was run three times, χ-1 and χ-1′ being kept at the same angle with drivers, those angles being the three staggered forms, −60, 60, and 180°.

The above protocol created a $12 \times 12 \times 12 \times 3$ data array. A ϕ–ω minimum-energy map was generated by selecting the low-energy structure for each ϕ–ω combination for all tested side-group angles and ψ/χ-6′ angles (Fig. 2). The torsion angles of ϕ and χ-1/χ-1′ for that low-energy structure are listed in Table I. The *relative* energies of the staggered linkage forms are shown in Table II.

The ability of the χ-1/χ-1′ side groups to populate other than the low-energy forms was tested by comparing the lowest energy conformer with the next highest energy conformer having a different χ angle (and any ψ angle) at each ψ and ω value. The energy difference between these two forms was then determined and the result was plotted (Fig. 3).

Run B: all the structures having steric energies within 10 kcal/mol of the Run A minimum were extracted and optimized separately without any restriction. After

TABLE I

Optimum ψ and χ-1/χ-1′ values from the Run A driver study [a]

ω (deg)	ϕ (deg)											
	−150	−120	−90	−60	−30	0	30	60	90	120	150	180
−150	−150	180	150	−150	180	180	−90	−120	150	−150	−90	180
	60	60	60	60	60	60	60	60	60	60	60	180
−120	180	−150	180	−150	120	−150	−150	150	150	−150	−90	−150
	60	60	60	60	60	60	60	60	60	60	60	60
−90	−150	180	150	150	−150	180	150	150	150	180	150	150
	60	−60	60	60	60	60	180	60	60	−60	−60	−60
−60	150	180	150	150	−150	180	180	150	150	90	150	180
	180	60	60	60	60	−60	60	60	60	180	60	60
−30	120	−150	120	−150	180	180	180	150	120	90	150	−150
	180	180	60	60	60	−60	180	60	60	180	180	60
0	−150	−150	180	−150	180	180	180	−150	−150	180	−90	150
	180	180	180	180	180	180	180	180	180	180	180	180
30	−150	180	90	−120	−150	90	90	60	90	−90	−120	120
	60	60	60	60	60	60	60	60	60	180	60	180
60	−150	180	−150	−150	180	180	60	60	−120	−90	180	150
	60	60	60	60	60	60	−60	−60	60	180	60	180
90	−150	−150	180	−150	180	180	60	−120	180	180	180	−120
	180	180	180	60	60	60	180	60	180	180	180	180
120	180	−150	150	120	180	180	150	150	180	180	180	150
	180	180	180	60	60	60	180	180	180	180	180	180
150	150	150	150	150	180	−90	180	150	180	180	150	150
	150	180	180	60	180	180	180	180	180	180	180	180
180	150	120	150	120	180	180	180	150	150	180	150	150
	180	60	180	60	−60	180	180	−60	60	180	−60	180

[a] For each ϕ and ω, the top value indicates the optimum ψ and the bottom value the optimium χ-1/χ-1′ angle.

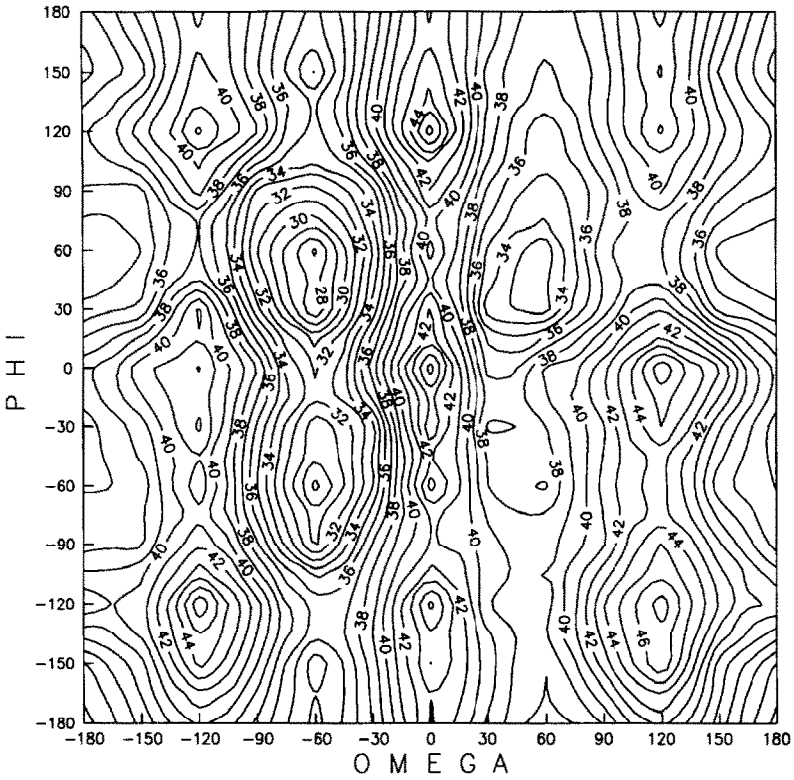

Fig. 2. $\phi-\omega$ Energy map from the dihedral angle driver study of ϕ, ψ, ω, χ-1′, and χ-6′, Run A. The point used at each value of ϕ and ω was the lowest-energy value for all χ-1/χ-1′ and ψ points. The values of ψ and χ-1/χ-1′ are shown in Table I.

optimization, all structures which had a steric energy within 5 kcal/mol of the lowest-energy form had torsion angles of $\psi = 46 \pm 4°$, $\psi = 166 \pm 5°$, and $\omega = -60 \pm 9°$. When the driver restrictions were removed, many structures relaxed to three low-energy forms, sometimes overcoming eclipsing barriers in the process. A list of those three resulting structures is given in Table III.

TABLE II

Relative energies (kcal/mol) of the nine staggered forms of ϕ and ω as found in Run A[a]

ϕ	ω		
	−60	60	180
−60	2	12	10
60	0	5	6
180	8	10	8

[a] Minimum energy of 26.86 kcal/mol at $\phi = 60$ and $\omega = -60°$.

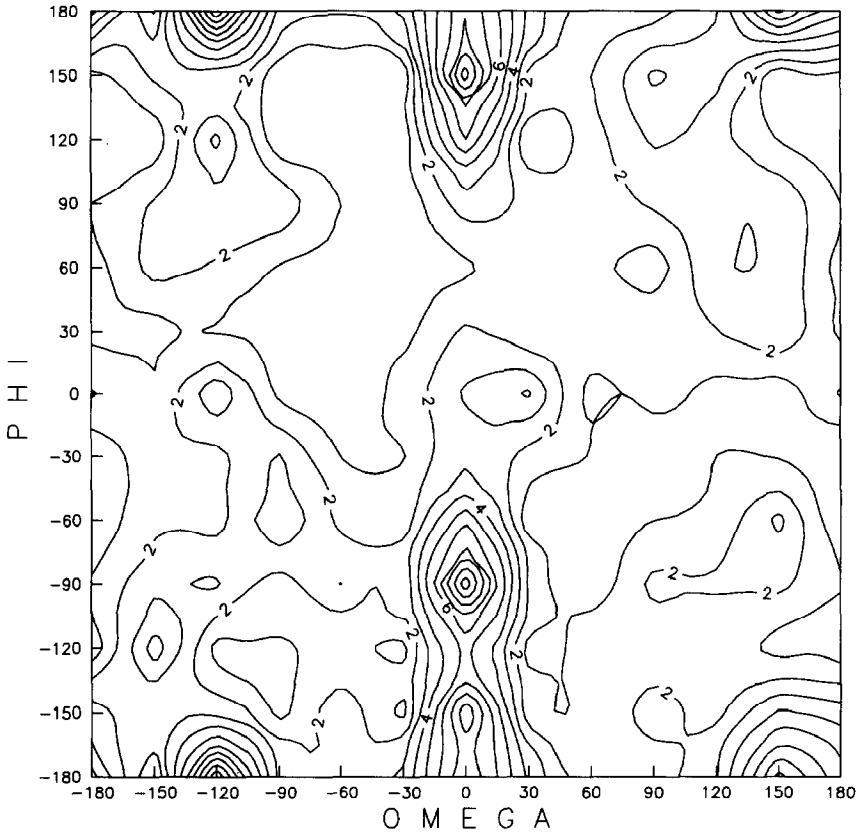

Fig. 3. The energy difference between the lowest and next-lowest energy for staggered forms of χ-1/χ-1′ at each $\phi-\omega$ point found in Run A. The lowest-energy χ-1 value is found in Table I.

Run C: starting with the lowest relaxed energy form found in Run B, χ-1, χ-1′, and χ-6′ were rotated separately through all staggered forms while ϕ, ψ, and ω were allowed to relax. Then each output structure was re-optimized without any restrictions (Table IV). The resulting lowest-energy structure was the global minimum structure (Fig. 4, Table V).

TABLE III

Run B results: three of the fully relaxed model structures derived from Run A results [a]

Angle (deg)						Energy (kcal/mol)
ϕ	ψ	ω	χ-1	χ-1′	χ-6′	
48.50	167.04	−57.73	−172.15	−177.79	−59.34	23.19
49.67	167.90	−55.79	57.88	46.35	−58.32	24.06
45.05	167.08	−64.29	−64.47	−67.02	−60.27	26.07

[a] The structures which were subjected to fully relaxed minimization were limited to those having a steric energy within 10 kcal/mol of the lowest energy found in Run A.

TABLE IV

Run C: search of different side-group orientations and global minimum [a,b]

Angle (deg)						Energy (kcal/mol)
ϕ	ψ	ω	χ-1	χ-1′	χ-6′	
48.73	160.91	−63.09	−64.32	−66.03	−58.26	24.85
47.53	162.51	−65.83	62.39	−66.16	−59.66	23.54
47.94	164.94	−60.44	−172.07	−65.78	−57.09	24.13
50.88	163.17	−63.58	−64.66	48.83	−59.68	24.62
49.76	164.54	−65.86	62.53	48.88	−61.09	23.32
49.48	167.11	−60.68	−172.06	48.19	−58.25	23.74
47.58	165.31	−61.82	−64.43	−176.82	−60.02	23.00
46.38	165.62	−65.37	61.64	−176.90	−61.45	22.02
47.58	166.05	−59.34	−172.56	−177.49	−58.39	23.12
50.35	163.84	−62.04	−65.92	−67.02	64.22	31.15
53.12	161.82	−62.41	64.39	−66.83	64.77	29.67
49.73	165.59	−62.28	−172.96	−66.72	64.11	29.58
52.35	164.67	−62.83	−66.31	49.60	65.00	31.38
56.59	161.84	−62.79	64.76	50.55	65.49	29.81
51.77	166.65	−62.34	−173.23	48.92	64.92	29.70
50.96	167.31	−60.04	−66.10	−176.43	65.30	28.47
51.62	166.91	−58.95	56.64	−176.69	65.93	28.05
50.99	166.45	−59.74	−174.30	−176.59	65.28	27.64
50.71	164.74	−60.63	−65.94	−72.10	176.78	30.88
53.97	158.48	−63.00	64.66	−66.74	177.98	28.51
52.08	165.62	−58.70	−174.16	−72.18	176.82	29.93
53.94	163.29	−62.07	−65.90	49.54	176.96	30.34
57.79	157.79	−63.86	64.83	51.17	177.38	28.57
56.34	171.57	−58.09	−172.59	48.53	177.18	28.39
51.10	163.56	−60.40	−65.81	−176.80	176.36	27.65
51.16	163.03	−60.00	56.07	−177.13	175.79	27.21
51.44	162.95	−59.79	−174.34	−176.96	176.33	26.77

[a] Table arranged in the order of increasing χ-6′, then χ-1′, then χ-1. [b] Average value: $\phi = 51.18 \pm 7$, $\psi = 164.31 \pm 7$, and $\omega = -61.70 \pm 4°$. [c] Global minimum.

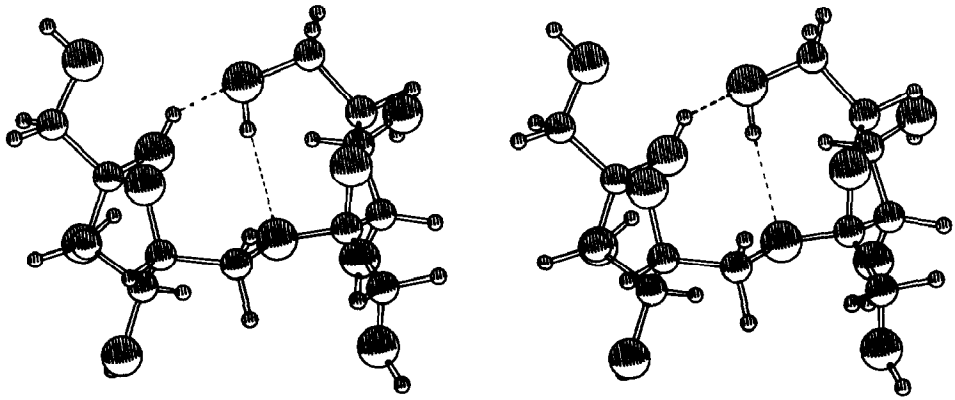

Fig. 4. Stereoview of global minimum levanbiose structure, steric energy = 22.02 kcal/mol. H-Bonds indicated with dashed lines. Table V contains the coordinates.

TABLE V

The coordinates of the global minimum structure as shown in Fig. 4

Atom	x	y	z
C-1	−4.44462	−2.81618	−0.79197
C-2	−3.39868	−3.29539	0.19291
C-3	−3.69968	−4.61440	0.86906
C-4	−2.83837	−4.51106	2.11106
C-5	−2.96878	−3.03008	2.43136
C-6	−1.78576	−2.42950	3.18136
O-1	−3.96199	−1.62772	−1.41847
O-5	−3.16675	−2.34743	1.20017
O-3	−3.28569	−5.70217	0.04641
O-4	−3.34699	−5.33228	3.15883
O-2	−2.15287	−3.41640	−0.48440
O-C2′	−0.59828	−2.66230	2.44244
HO-1	−4.56408	−1.39374	−2.10308
HO-2	−1.91187	−2.54273	−0.73874
HO-3	−2.52243	−5.39884	−0.42003
HO-4	−3.23859	−6.22550	2.87984
C-1′	0.76485	−1.87258	4.33858
C-2′	0.53129	−1.90385	2.83525
C-3′	1.75684	−2.44719	2.11366
C-4′	1.54663	−1.90796	0.71651
C-5′	0.97672	−0.53196	1.03627
C-6′	0.00000	0.00000	0.00000
O-1′	1.02734	−3.20557	4.77961
O-5′	0.33275	−0.61251	2.30330
O-3′	1.80143	−3.87247	2.14214
O-4′	2.78106	−1.82392	0.00907
O-6′	−1.10345	−0.89818	−0.11530
HO-1′	1.19332	−3.18189	5.70552
HO-3′	1.52928	−4.13165	3.00811
HO-4′	3.05294	−2.70816	−0.16852
HO-6′	−0.96086	−1.60697	0.49332
H-1	−4.62338	−3.57346	−1.58883
H-1	−5.40949	−2.58038	−0.28796
H-3	−4.78312	−4.72093	1.11174
H-4	−1.78612	−4.81495	1.90366
H-5	−3.89840	−2.87205	3.03206
H-6	−1.94872	−1.33465	3.31334
H-6	−1.70489	−2.92747	4.17503
H-1′	−0.08687	−1.46022	4.92325
H-1′	1.65808	−1.25676	4.59059
H-3′	2.69818	−2.05168	2.56399
H-4′	0.84748	−2.54880	0.13120
H-5′	1.81651	0.19602	1.15261
H-6′	0.47974	0.08405	−1.00203
H-6′	−0.39944	0.99559	0.30206

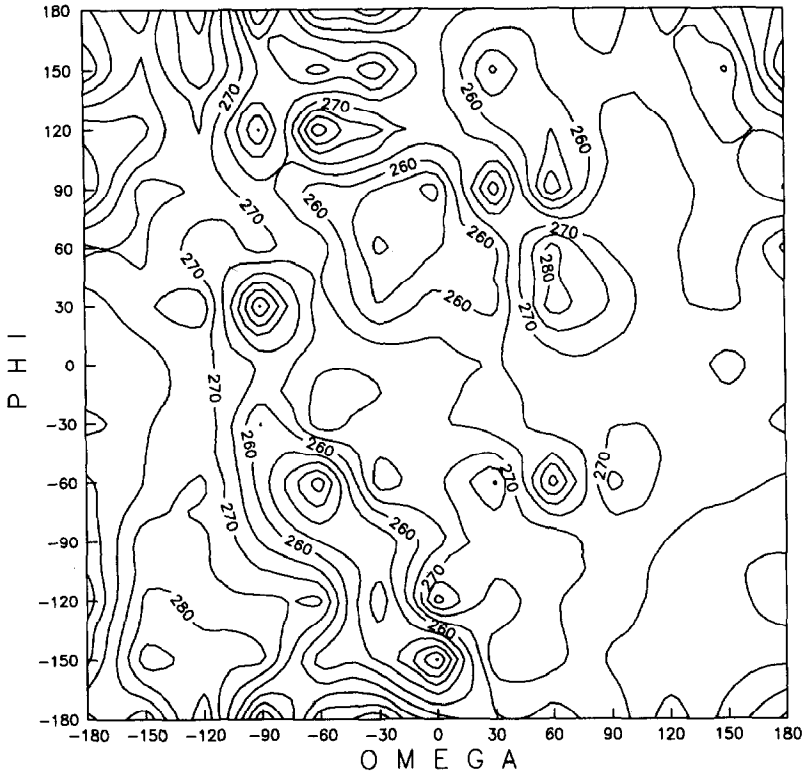

Fig. 5. Pseudorotation map for Fru-1 (Fig. 1). Values on the contour levels indicate the Cremer–Pople phase angle of pseudorotation, ϕ_2.

For each structure generated in Run A, the Cremer–Pople puckering parameters of the sugar rings were assessed with a program written by Larry Madsen. Contour plots of the calculated Cremer–Pople phase angle (ϕ_2) are presented in Figs. 5 and 6.

The global minimum structure (Run C) was used as the input structure for comparison with the optimum structure found by other programs: MM3 and MOPAC (AM1, MNDO, and MINDO/3). The results are listed in Table VI.

The structures from run A that were within 10 kcal/mol of the run minimum were used to create tetramers from which N and H values of the potential polymers could be calculated. For instance, a tetramer was created where all ϕ angles were set to $-60°$, all ψ angles to 150°, all ω angles and the one χ-6 angle to 60°, and all χ-1 angles to $-60°$, using the dimer with the same torsion angles. Internal coordinates of the potential polymer were determined from distances and angles between the same atom on each repeating unit, i.e., C-2, and this information was applied to determine N and H (ref. 17). An energy of each tetramer was

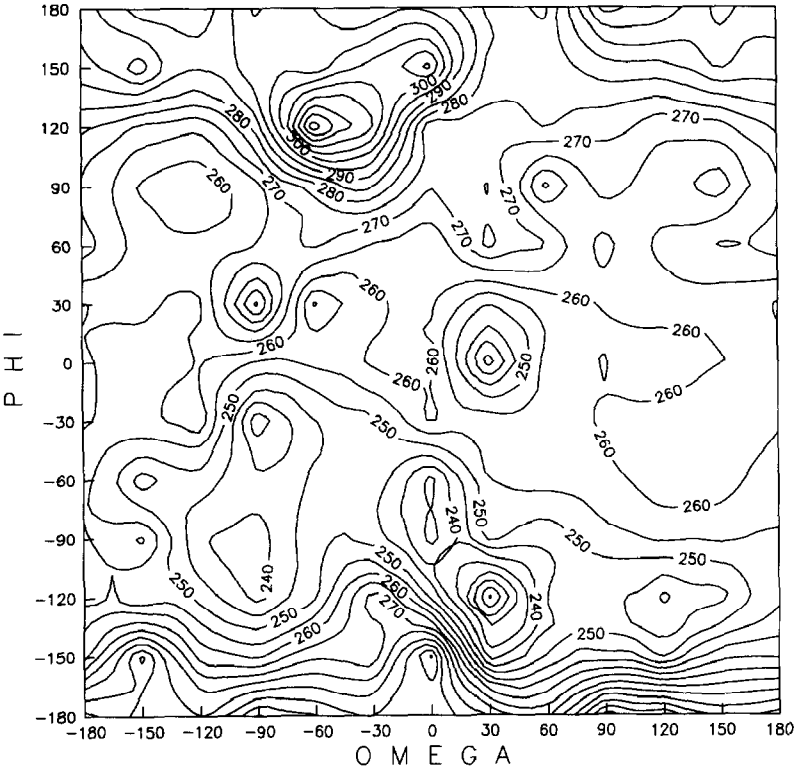

Fig. 6. Pseudorotation map for Fru-2 (Fig. 1).

TABLE VI

Torsion angles of the global minimum structure as optimized using different molecular modeling programs

Method	Angle (deg)					
	ϕ	ψ	ω	χ-1	χ-1′	χ-6′
MM2(87)	46.38	165.62	−65.37	61.64	−176.90	−61.45
MM3	47.07	165.75	−66.62	63.57	−174.01	−65.22
AM1	46.85	172.87	−48.81	70.92	160.98	−65.42
MNDO	44.08	172.91	−61.18	63.93	179.08	−61.24
MINDO/3	60.47	−174.40	−85.23	65.69	−167.52	−89.33

determined using PCMODELs * MMX force field. The results are listed in Tables VII and VIII.

* Serena Software, Bloomington, IN 47402, USA.

TABLE VII

The N and H analysis of the 15 lowest-energy structures from Run A. The dimer energy is calculated by MM2 and the tetramer energy by MMX. The pitch is the product of N and H

Name [a]	Dimer energy (kcal/mol)	N	H	Pitch	Tetramer energy (kcal/mol)
LGBRVY	26.8616	2.2217	1.4187	3.152	3367.24
LGBRUZ	27.0104	2.4997	1.4997	3.7488	5231.19
LGARVY	27.184	2.2083	1.4173	3.13	3277.25
LGARUZ	27.4668	2.5544	1.3882	3.5462	4755.14
LGBRRY	28.7243	−2.3949	1.553	3.7193	3607.22
LGCRUZ	28.8074	2.5162	1.4088	3.5448	6121.24
LGCRVY	28.9721	2.1889	1.3872	3.0364	3518.25
LGARVZ	29.6174	2.3581	2.0138	4.7487	1595.68
LGARUY	29.6946	2.6253	0.9394	2.4663	5203.51
LGBRRX	29.79	−2.8859	2.0472	5.9079	270.92
LGBRUY	29.968	2.4727	0.9719	2.4031	7046.75
LGBRVZ	30.0304	2.2956	2.0885	4.7943	249.29
LGBRSN	30.3557	2.8967	0.8312	2.4077	8120.23
LGARRZ	30.4413	−2.417	1.1216	2.711	6832.15
LGBRQY	30.7639	−2.6556	2.2112	5.8721	1635.08

[a] The 3rd character indicates χ-1 (A = −60, B = 60, and C = 180°), the 4th character indicates ω and χ-6, the 5th character indicates ϕ, and the last character indicates ψ (N = −150, P = −120, Q = −90, R = −60, S = −30, T = 0, U = 30, V = 60, W = 90, X = 120, Y = 150, and Z = 180°).

TABLE VIII

The N and H analysis of the 15 lowest-energy structures of the tetramers created from Run A. The dimer energy is calculated by MM2 and the tetramer energy by MMX. The pitch is the product of N and H

Name [a]	Dimer energy (kcal/mol)	N	H	Pitch	Tetramer energy (kcal/mol)
LGCZVZ	34.0083	−3.1443	2.4282	7.6348	12.45
LGCVVZ	36.3894	−2.4901	4.1703	10.3846	13.29
LGCYWZ	36.3987	−3.3969	2.0891	7.0967	17.09
LGCZUZ	34.2276	−2.9055	3.4024	9.8858	18.82
LGAZVZ	35.2838	−3.2099	2.3619	7.5814	18.95
LGAZVY	33.1462	−2.6724	2.8724	7.6761	18.97
LGCWWZ	36.6521	−3.0644	3.6313	11.1275	19.65
LGCYVZ	34.1744	−3.1644	3.3194	10.5038	19.92
LGCWWN	36.8121	−3.2272	3.2423	10.4636	20.37
LGAVVY	36.5285	−2.2947	4.1052	9.42	20.97
LGCZVY	33.6976	−2.551	2.786	7.1072	21.2
LGAVVZ	36.4122	−2.4944	4.2338	10.5609	21.61
LGCZVN	36.4217	−4.0256	1.9275	7.7593	21.76
LGCVVP	33.7146	−2.7876	3.7274	10.3906	23
LGCYVY	33.7596	−2.5481	3.4236	8.7237	23.15

[a] See Table VII for an explanation of the name.

RESULTS AND DISCUSSION

The force field used by MM2(87) is one of the best available for carbohydrates. Parameters were incorporated for carbohydrates in the 1985 version [18] of the program to compensate for the varied bond length associated with anomeric centers and retained in this version. In addition, the treatment of H-bonding was refined in the 1987 version [19]. However, because the calculations are carried out on isolated or gas-phase molecules, there will be some differences with solution data. The internal dielectric constant correction factor had no effect and was not used.

ψ Analysis.—As observed in previous work on inulobiose [7], the antiperiplanar arrangement of the three linkage bonds is preferred for ψ, except for some strained conformations. This is also true in the case of **1**.

In Run A, a notable deviation from this rule is the conformation where ϕ, ψ, and ω are all at 60°, although this a relatively high-energy structure. Its steric energy is about 5 kcal/mol higher than the lowest-energy structure in the energy contour map, but it is 3.3 kcal/mol lower than the one with ϕ and ω at 60° and ψ at 180°. Having ψ at 60° when setting both ϕ and ω to 60° minimizes the interaction between the CH_2 group on the linkage and the primary alcohol group on C-2′. When this structure was optimized without any restriction, it relaxed to $\phi = 41.2$, $\omega = 56.6$, and $\psi = 66.5°$ where the steric energy is ~ 9 kcal/mol higher than the global minimum structure. Similar cases can also be found when ψ is at 90 or −90°, but these are not at local minima (Fig. 2 and Table I) nor do they have significant populations based on Boltzmann distribution.

ϕ and ω Analysis.—In the ϕ–ω energy map generated by the driver study, Run A (Fig. 2), the staggered positions are the preferred angles for both ϕ and ω, giving the map roughly threefold symmetry in both dimensions. The optimal value for ϕ and ω are 60 and −60°, respectively, and the energy found at that point was 26.9 kcal/mol. The relative energies of all the staggered forms are listed in Table II.

The lowest energy is found when $\phi = 60°$. When ϕ is at −60°, a strong interaction between the linkage CH_2 group and the OH group on C-3′ keeps the steric energy high. When ϕ is at 180°, the CH_2 in the linkage is placed on top of the second fructofuranose ring.

Since there are fewer substituents on ω, one would expect less preference for any staggered angle of ω, while −60° is clearly preferred. (See Table II). This is due to the hydrogen bonding between the hydrogen on O-2 and O-6′ (bond length ~ 1.93 Å). When ω equals 60°, hydrogen bonding can still occur, but this conformer has a steric energy of 5 kcal/mol higher than the one with ω at −60°. The ω angle is much more rigid than that of inulobiose [7], where the ω angle at 180 and 60° has steric energies only 2 and 4 kcal/mol, respectively, higher than ω at −60°.

Side-group orientation.—In Run A, χ-1 was forced to be equal to χ-1′ and ω to χ-6′ for the purpose of polymer extrapolation. In this study, one can see by comparing Table I and Fig. 2 that in the energetic valleys, at $\omega = -60°$ and where ϕ was at 60 or $-60°$, then the preferred angle of the χ-1 side groups was 60°.

Looking at the structure with preferred linkage angles found in Run A and refined in Run B ($\phi \approx 60$, $\psi \approx 180$, and $\omega \approx -60°$), our study of all side-group orientations in Run C showed that the energy differences between all χ-1 and χ-1′ combinations are within 3 kcal/mol while variation in the χ-6′ angle gives an energy difference of at least 6 kcal/mol higher than the lowest energy (Table IV). We were initially surprised at the differences in flexibility of these two similar groups, but, as noted above, there is an H-bond between HO-2 and O-6 and that can explain why $-60°$ is strongly preferred. The global minimum was found when χ-1 = 61.6, χ-1′ = −176.9, and χ-6′ = −61.5°, with a steric energy = 22.01 kcal/mol. A stereoview of this structure is presented in Fig. 4, and the coordinates are listed in Table V.

The orientation of the secondary side groups is not as important in the case of fructofuranose rings, due to the fact that they are not in a position to form H-bonds, as is the case of the glucopyranose ring.

Ring conformation.—All possible conformations of the furanose ring can be systematically described by the use of a pseudorotational wheel [20,16], and positions on the wheel can be indicated with the E/T notation [21] or the related Cremer–Pople pseudorotational phase angle ϕ_2 for fructofuranoses.

French and Tran [16] reported a ring-puckering analysis of fructofuranose. In their study, two minima were found for the β form, the primary near the ${}^{4}_{3}T$ conformation ($\phi_2 = 270°$), and a secondary (2.6 kcal/mol higher) near the ${}^{3}_{4}T$ conformation ($\phi = 90°$).

Our starting structure has the ring conformation of ${}^{4}_{3}T$ (ϕ_2 is 266 and 258° for Fru-1 and -2, respectively). The phase angle of ring puckering was monitored during Run A. It was found that the starting ring conformation, the ${}^{4}_{3}T$ form, was retained except when a high steric strain was encountered.

The distortion of Fru-2 was slightly greater than that of Fru-1, the range of ϕ_2 for Fru-1 being 234–289° (Fig. 5) and 214–328° for Fru-2 (Fig. 6). It is clear from Figs. 5 and 6, and intuition would predict, that changes in the torsion angle of ω or ϕ more strongly affect the ring to which it is attached, Fru-1 and Fru-2, respectively.

For the global minimum structure, the ϕ_2 is 267 for Fru-1 and 258° for Fru-2. In all of the low-energy structures, no southern conformer was found. The puckering parameters calculated from X-ray diffraction data for the levanbiose moiety of 6-kestose [9] are 273 and 252° for Fru-1 and 2, respectively.

Compared to a recent study of inulobiose [7], ring-shape changes observed in levanbiose are much greater in the linkage analysis. This may be due to the differences between the MM2(85) program used in inulobiose study and MM2(87) program used here. MM2(87) specifically accounts for hydrogen bonding, and

inter-residue hydrogen bonding appears to have a large effect on the conformation changes on both rings in this study.

Comparison of other computational methods with global minimum structure.—The global minimum structure was subjected to reoptimization using other programs to see what differences might be observed in the structural geometry. Calculations were carried out with MM3 [22], and three methods in MOPAC [23], AM1, MNDO, and MINDO/3. The results are listed in Table VI. The comparisons are interesting, but semi-empirical methods have some serious problems with carbohydrates (AM1 incorrectly predicts that glucopyranose prefers the $^1C_4$ conformation) [24].

Determination of N and H values.—The lowest dozen or so energy structures found for the dimer will extrapolate to polymers with such low values for H that a large number of short contacts appear, and the calculated energy for the tetramers is extremely high. However, examination of all structures in Run A within 10 kcal of the minimum produces many viable polymers. Comparisons of the low-energy dimers, Table VII, with the low energy tetramers, Table VIII, indicate that the dimers prefer to have ω in the $-60°$ angle, but the tetramers prefer ω in the 180° form. On the other hand, the positions of ϕ do not seem to be very different, and of course in every case the ψ angle is near antiperiplanar.

CONCLUSIONS

This study points out that modeling can explore questions which cannot be studied experimentally. Here we have analyzed the interactions between two (2 → 6)-β-linked fructofuranoses, at least to a first-order approximation, and such a study would be appear to be difficult if not impossible to carry out experimentally. These results will be useful in the analysis of larger compounds which contain the same linkage, especially 6-kestose and related oligomers, as well as levan polymer. Our initial driver study (Run A) defines what conformational space is accessible for potential levan polymers that have the same internal geometry in each monomer unit — in terms of the linkage angles, ϕ, ψ, and ω.

For dimers of five-membered rings with three-bond linkages, the lowest-energy structures have an antiperiplanar angle at the central bond (ψ). The other two angles, ϕ and ω, have energetic valleys at the three staggered positions, but in levanbiose, intramolecular hydrogen bonding creates a strong preference for ϕ and ω at $+60$ and $-60°$, respectively. The side-group orientations affect the steric energy depending on the ϕ–ω combination, but are not generally important except when intramolecular H-bonds are involved. The ring shape deviates only slightly from the ^3_4T form found in the monomer.

ACKNOWLEDGMENTS

We thank Dr. Alfred French for any stimulating discussions and assistance with the MM3 calculations, and the Computing Services at Tulane University and at the

University of California, Davis, for providing computing facilities. We also thank the University of California, Davis, Vice Chancellor-Research for partial financial support.

REFERENCES

1 S. Hestrin, D.S. Feingold, and G. Avigad, *Biochem. J.*, 64 (1956) 340–351.
2 B. Andersen, *Acta Chem. Scand.*, 21 (1967) 828–829.
3 G. Hendry, *New Phytol.*, 106 (1987) 201–216.
4 H.G. Pontis, *J. Plant Physiol.*, 134 (1990) 148–150.
5 Y.W. Han, *Adv. Appl. Microbiol.*, 35 (1990) 171–194.
6 A.D. French, *Carbohydr. Res.*, 176 (1988) 17—29.
7 T.M. Calub, A.L. Waterhouse, and A.D. French, *Carbohydr. Res.*, 207 (1990) 221–235.
8 R.H. Marchessault, T. Bleha, Y. Deslendes, and J.T. Revol, *Can. J. Chem.*, 58 (1980) 2415–2417.
9 V. Ferretti, V. Bertolasi, G. Gilli, and C.A. Accorsi, *Acta Crystallogr., Ser. C*, 40 (1984) 531–535.
10 H.C. Jerrel, T.F. Conway, P. Moyna, and I.C.P. Smith, *Carbohydr. Res.*, 76 (1979) 45–57.
11 J. Liu, A.L. Waterhouse, and N.J. Chatterton, *Carbohydr. Res.*, 217 (1991) 29–42.
12 D.S. Feingold and M. Gehatia, *J. Polym. Sci.*, 23 (1957) 783–790.
13 E. Newborn and S. Baker, *Carbohydr. Res.*, 6 (1968) 165–170.
14 J. Liu and A.L. Waterhouse, unpublished results.
15 A.D. French, V. Tran, and S. Perez, *ACS Symp. Ser.*, 430 (1990) 191–212.
16 A.D. French and V. Tran, *Biopolymers*, 29 (1990) 1599–1611.
17 T. Miyazawa, *J. Polym. Sci.*, 55 (1961) 215–231.
18 L. Nørskov-Lauritsen and N.L. Allinger, *J. Comput. Chem.*, 5 (1984) 326–335.
19 N.L. Allinger, R.A. Kok, and M.R. Imam, *J. Comput. Chem.*, 9 (1988) 591–595.
20 A.D. French, *J. Plant Physiol.*, 134 (1989) 125–136.
21 W. Saenger, *Principles of Nucleic Acid Structure*, Springer-Verlag, New York, 1984, p. 17.
22 N.L. Allinger, M. Rahman, J.H. Lii, *J. Am. Chem. Soc.*, 112 (1990) 8293–8307.
23 J.J.P. Stewart, *QCPE*, 9 (1989) 99–100.
24 A.D. French, personal communication.